metals

MDPI

Article

Comparison of the Dislocation Structure of a CrMnN and a CrNi Austenite after Cyclic Deformation

Rainer Fluch [1,*], Marianne Kapp [1], Krystina Spiradek-Hahn [2], Manfred Brabetz [2], Heinz Holzer [3] and Reinhard Pippan [4]

1 Product and Process Development, voestalpine BÖHLER Edelstahl GmbH & Co KG, 8605 Kapfenberg, Austria
2 AGD Seibersdorf, University of Leoben, 2444 Seibersdorf, Austria
3 Österreichisches Gießerei-Institut, University of Leoben, 8700 Leoben, Austria
4 Erich Schmid Institute of Materials Science, Austrian Academy of Sciences, 8700 Leoben, Austria
* Correspondence: rainer.fluch@bohler-edelstahl.at; Tel.: +43-3862-20-36062

Received: 14 May 2019; Accepted: 19 June 2019; Published: 13 July 2019

Abstract: In the literature, the effects of nitrogen on the strength of austenitic stainless steels as well as on cold deformation are well documented. However, the effect of N on fatigue behaviour is still an open issue, especially when comparing the two alloying concepts for austenitic stainless steels—CrNi and CrMnN—where the microstructures show a different evolution during cyclic deformation. In the present investigation, a representative sample of each alloying concept has been tested in a resonant testing machine at ambient temperature and under stress control single step tests with a stress ratio of 0.05. The following comparative analysis of the microstructures showed a preferred formation of cellular dislocation substructures in the case of the CrNi alloy and distinct planar dislocation glide in the CrMnN steel, also called high nitrogen steel (HNS). The discussion of these findings deals with potential explanations for the dislocation glide mechanism, the role of N on this phenomenon, and the consequences on fatigue behaviour.

Keywords: austenitic high nitrogen steel (HNS); cold deformation; fatigue

1. Introduction

In the last twenty five years, a lot of research has been conducted regarding interstitially alloyed high nitrogen steels (HNS), especially on high nitrogen austenitic steels, which still have not emerged from their status as highly specialised products for niche markets where a combination of strength, toughness, corrosion resistance, and non-magnetic behaviour is required. Those classical applications are medical implants, drill collars, and retaining rings. To achieve the high strength values required for these applications (R_m > 1000 MPa), a further characteristic of that alloying system is taken advantage of: its exceptional work hardening rate. As a consequence, the alloys are often deployed in a work hardened condition. Additionally, it is common requirement for all these applications that the material has to withstand cyclic loads. Therefore, fatigue resistance is an additional important characteristic of these alloys.

In the case of austenitic steels, the arrangement of dislocations during cyclic deformation is of crucial significance to their fatigue behaviour. The first attempts to define this behaviour in alloys with face centered cubic (FCC) microstructure through their dislocation structures independent of the stacking fault energy (SFE) were done by Feltner and Laird [1] and Lukáš and Klesnil [2]. They distinguished between wavy slip for high SFE and planar slip for low SFE materials. Wavy slip implies that cross slip of dislocations can occur easily; in the case of planar slip, cross slip is impeded. Figure 1a shows the "dislocation distribution map" proposed by Lukáš and Klesnil [2] (from Reference [3]).

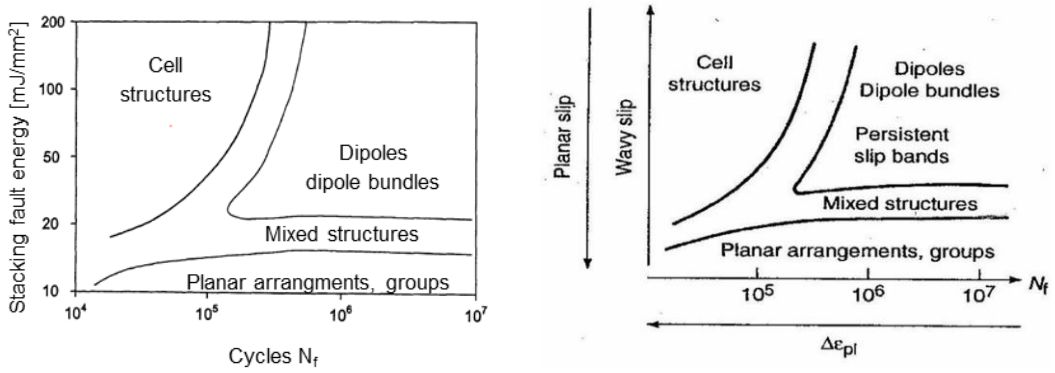

(**a**) (**b**)

Figure 1. (**a**) Dependence of stacking fault energy on cyclic slip mode and fatigue life [3], with permission from DGM, 2019; (**b**) modified diagram proposed by Mughrabi [4], with permission from Elsevier, 2019.

Parallel to this observation, many authors have reported that nitrogen reduces the stacking fault energy in austenitic steels [5–9]. The majority of those investigations have been carried out on CrNi-austenitic steels [10–12]. However, there have been other studies which described an increase of stacking fault energy with N [13], or even a non-monotonous dependence [14]. Moreover, in recent publications it was stated that—in contrast to twinning induced plasticity (TWIP) and transformation induced plasticity (TRIP) steels—for the calculation of SFE in austenitic alloys containing N, the existing methods are is still not reliable [15–17].

Therefore, as far as N is concerned, no clear relationship with the stacking fault energy could be established. A different approach to explain the planar dislocation behaviour of austenitic steels is through short range ordering (SRO), as was already mentioned by Douglas et al. [18] in 1964. Gerold and Karnthaler stated that there might be an overestimation of the influence of SFE on the mobility of dislocations [19]. They mentioned that SRO leads to a glide plane softening effect in solid solution. SRO has also been discussed by Grujicic et al. [20] and Gavriljuk and Berns [21] in connection with high nitrogen austenitic steels, which would explain the planar slip behaviour of high nitrogen austenitic steel and, as a consequence, its high work hardening rate. Based on these findings, Mughrabi suggested a modified version of Figure 1a where he replaced the stacking fault energy on the *y*-axis, indicating that wavy slip is dominating higher in the diagram, and planar slip is preferred towards the bottom of the diagram (Figure 1b) [4].

Comparing the two alloying concepts for austenitic stainless steels, different mechanisms for dislocation slip can be identified:

- Wavy slip due to high SFE is expected for CrNi alloys.
- Planar slip appears in CrMnN alloys which show beside a lower SFE also SRO owing to the interstitially alloyed nitrogen

The goal of the investigation was to analyse the dislocation slip behaviours of a CrNi alloy and a CrMnN alloy in a cold worked (CW) condition under cyclic loading.

2. Materials and Methods

2.1. Test Materials

The investigated materials were a CrNi alloy, of the standard austenitic grade UNS S31673, and a CrMnN alloy. The exact chemical composition can be found in Table 1. Additionally, the SFE values

were calculated with formula (1) from Reference [22], which Noh et al. [23] found to be the most adequate for different CrNiMnN alloys.

$$SFE = 5.53 + 1.4[Ni] - 0.16[Cr] + 17.1[N] + 0.72[Mn] \quad (1)$$

For CrMnN, the SFE = 35 $mJ \cdot m^{-2}$, which is a high value and would assume a cellular gliding for dislocations (Figure 1a). This would be in contrast to the above mentioned literature findings where mainly planar glide was reported for CrMnN steels.

The rods of the test materials were hot rolled to a 26.5 mm diameter, solution annealed (SA), and machined. Cold deformation was performed by cold drawing with a reduction of area of 14%, which resulted in residual tensile stresses in the tangential and also axial directions. The residual stresses have been observed by spring back after cutting exposure samples but have not been measured. The grain size of the CrMnN steel was approximately 40 µm, and the grain size of the reference grade CrNi was approximately 80 µm [12]. No precipitations were detected. The mechanical properties of the tested materials in solution annealed and cold worked (CW) states at room temperature under atmospheric conditions are presented in Table 2.

Table 1. Chemical composition of the test grades in wt%.

Grade	%C	%Mn	%Cr	%Mo	%Ni	%N	SFE [$mJ \cdot m^{-2}$]
CrNi S31673	<0.04	1.80	17.50	2.80	14.70	0.10	26
CrMnN	<0.04	23.00	21.10	0.30	1.50	0.85	35

Table 2. Mechanical properties of tested grades in solution annealed (SA) and cold worked (CW) condition at room temperature.

Grade	Condition	$R_{p0.2}$ [MPa]	R_m [MPa]	A_5 [%]
S31673	SA	410	637	54
	CW	653	718	32
CrMnN	SA	563	949	62
	CW	941	1165	38

2.2. Fatigue Experiments

A Rumul Testronic 8601/44 resonant testing machine with a nominal load of 100 kN was used. The sample geometry can be gathered from Figure 2.

As testing conditions, the following parameters were chosen:

Frequency: $f \approx 170$ Hz
Temperature: $T = 23$ °C
Max. load cycles: $N = 10^7$
Stress ratio: $R = 0.05$

A resonant testing machine reacts to changes in the system, like cracks, by a shift in the natural resonance. Therefore, a frequency drop of 0.2 Hz was defined for the shutdown parameter. The fatigue limit was set as the maximum stress σ_{max} where three specimens did not show rupture after 10^7 cycles. In order to avoid a rise in temperature caused by the high frequency during cycling in the gauge length, the sample geometry was adapted to an hourglass-shaped gauge length with a radius of 40 mm (R40). Additionally, the samples were purged with air for cooling. The maximum temperature measured with an emission-adsorption pyrometer during cycling was 60 °C. No difference between the two alloys concerning heating behaviour could be detected.

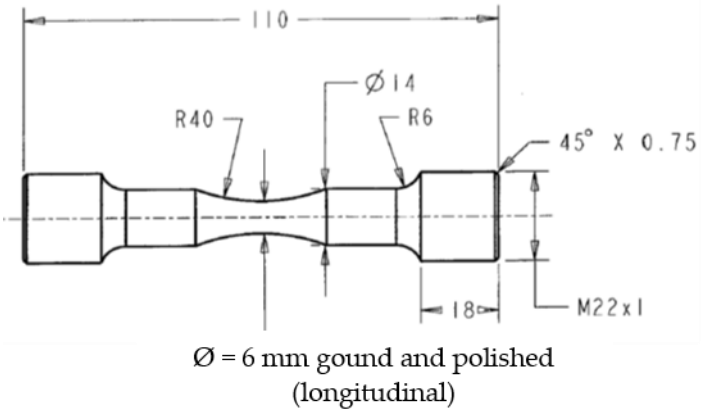

Figure 2. Drawing of the sample geometry.

2.3. TEM Investigations

The electron microscopic investigations have been carried out on thinned foil of the cross section of cold worked fatigue specimens with a transmission electron microscope Philips CM20 STEM and Tecnai F20 (high resolution Philips, FEI Company, Eindhoven, the Netherlands). The acceleration voltage was 200 kV. Thinning was achieved by mechanical thinning followed by electrolytic polishing. The samples were taken transverse to the axis, one from the grip section as an unloaded reference and one from the gauge section after 10^7 cycles. The CrNi sample was loaded with a maximum stress of 446 MPa, and the CrMnN sample with 526 MPa. The dislocation structure was analysed by TEM with bright and dark field imaging. To determine the crystallographic parameters, electron diffraction was applied.

3. Results and Discussion

3.1. Fatigue Experiments

Figure 3 displays the fatigue results of S31673 in the solution annealed and cold worked condition. The specimen which lasted till 10^7 cycles did not show rupture as the loading set up shut down after that number of cycles. The fatigue limit for the 14% CW specimen was about 50 MPa higher than for the solution annealed specimen. This value represents well the curve of the CW material, which seems almost parallel to the solution annealed curve in the tested area. Considering the $R_{p0.2}$ value—often looked to as the reference strength for the fatigue limit, and which is 243 MPa higher for the CW than for the SA condition—it is obvious that a softening of the CW material occurs during cyclic loading. This softening of cold hardened austenitic steels has been described in the literature [24–26] and has been attributed to the reversibility of dislocation slip.

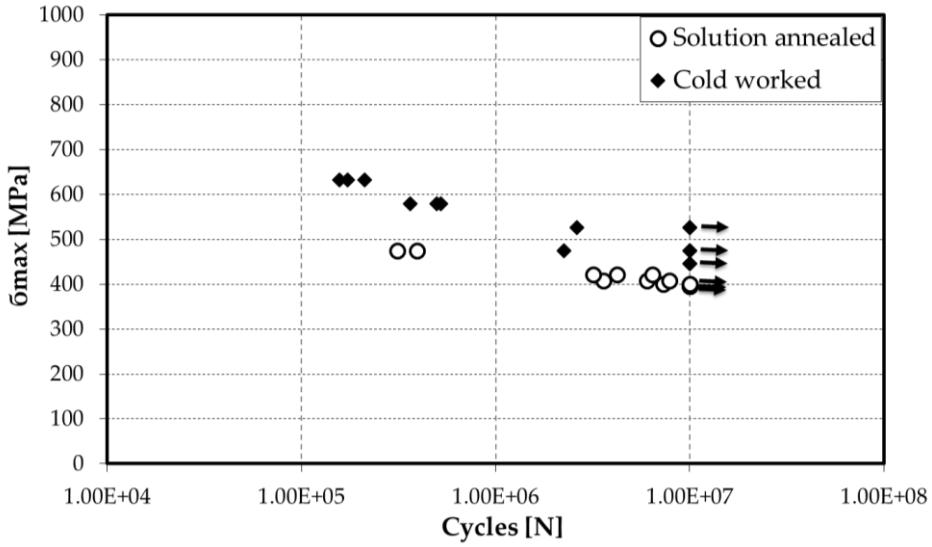

Figure 3. Plot of an S-N curve for S31673 at room temperature in the solution annealed and cold worked condition.

As expected, the CrMnN grade showed higher fatigue limits (>500 MPa, Figure 4) than S31673 since this grade possesses higher strength owned especially to the high interstitial alloyed N content. Although $R_{p0.2}$ of the CW material is 378 MPa higher, the fatigue limit at 10^7 cycles is not significantly higher than for the SA material. This implies that the reduction of the fatigue strength relating to $R_{p0.2}$ of cold worked material during cycling loading is more pronounced than for the CrNi grade. As mentioned earlier, this occurrence can be explained by the different dislocation slide behaviour of the two alloys, which leads to a higher reduction of dislocation density in the CrMnN steel. Nonetheless, at lower cycle numbers (e.g., 5×10^6) the cold worked CrMnN material shows higher fatigue stress values than the SA material.

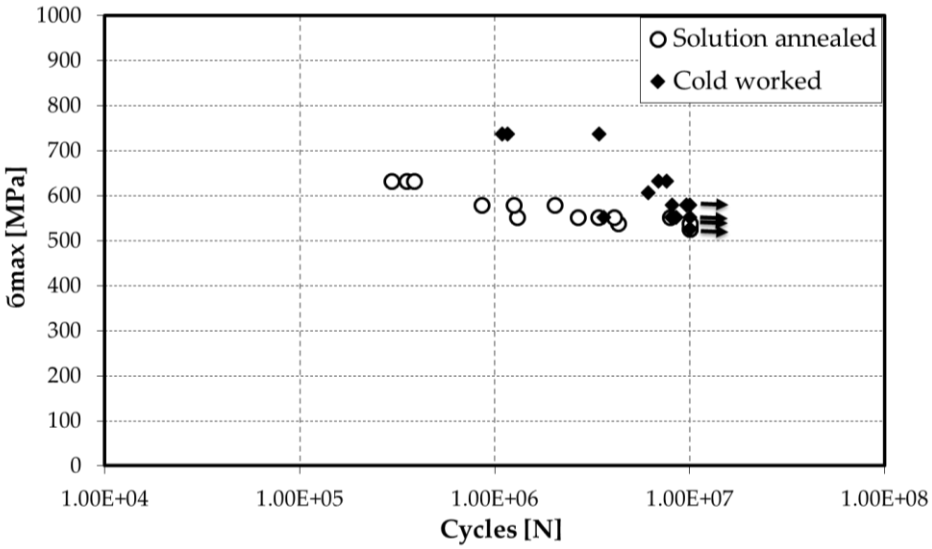

Figure 4. Plot of an S-N curve for CrMnN at room temperature in the solution annealed and cold worked condition.

3.2. TEM Investigations

To get a better understanding of the fatigue results, and to gain insight of the dislocation structures, TEM investigations have been carried out. The main points of interest were the cold deformed specimens and the different behaviour of the two alloying systems, CrNi and CrMnN, under cyclic

loading. Thus, the TEM investigations were executed on a S31673 and a CrMnN fatigue sample, both previously 14% cold worked.

The images of the samples taken from the unloaded head of the cold worked fatigue samples show the following microstructural features:

S31673 exhibits a high dislocation density and, in some areas, twinning with tendencies of cell formation between the twins (see marked area in Figure 5a). The twins are relatively broad and can be found in two orientation systems. To some extent, planar slip is also recognizable.

The dislocation density in CrMnN specimen is significantly higher than in the CrNi grade, and the dislocations are arranged along planar dislocation glide systems which constitute the predominant structure Figure 5b. The glide systems are arranged in three directions parallel to the {111} planes. Additionally, a high twin density can be found where the twins are thin compared to S31673.

To investigate the influence of the cyclic load on the dislocation structure of the 14% CW material, samples from the gauge length were investigated.

In the S31673 sample, more distinct cell structures were observed (see Figure 5c). Only residuals of the planar slip system with a low dislocation density in the area between can be found compared to the images of the unloaded S31673 sample.

No obvious differences could be found in the fatigued CrMnN specimen compared to the unloaded CrMnN specimen (from the head) (Figure 5d). The planar glide bands are arranged along the {111} planes. To some extent, there is room for the interpretation that the planes are not as defined as in the unloaded specimen. In Figure 5e, no distinct glide bands are visible, but a dislocation accumulation in one direction (red arrow) can be seen. The red ellipses indicate the beginnings of cell formation.

To summarise the findings of the TEM investigations, it can be said that there is a clear difference in the dislocation structures between the two alloying systems in the cold worked condition. S31673 shows a pronounced cell structure of the cold deformed material, which is caused by wavy slip and is attributed to the high stacking fault energy of CrNi-alloys. Under cyclic load, this dislocation structure is further amplified. Whereas for the cold worked CrMnN grade, a dominant planar dislocation arrangement occurs, which can be found in both states and is attributed mainly to short range ordering. This is in contrast to the results of the calculation of the SFE in Table 1, where the CrMnN alloy has the higher SFE with 35 $mJ \cdot m^{-2}$ compared to CrNi with SFE = 26 $mJ \cdot m^{-2}$. This proves that calculating the SFE is not a practicable way to estimate the gliding behaviour of N alloyed steels.

On the one hand, this planar slip is responsible for the high cold hardening rate [21], but in the case of cyclic loading, it has been suggested [27] that this planar dislocation arrangement promotes the reversibility of dislocation glide and, in consequence, to the annihilation of dislocations, which could justify the distinct cyclic softening of the tested CrMnN. Nevertheless, a softening occurs also in the case of S31673 considering that Rm rises 130 MPa from the solution annealed to the cold worked condition, whereas the fatigue limit σ_{max} increases only about 50 MPa.

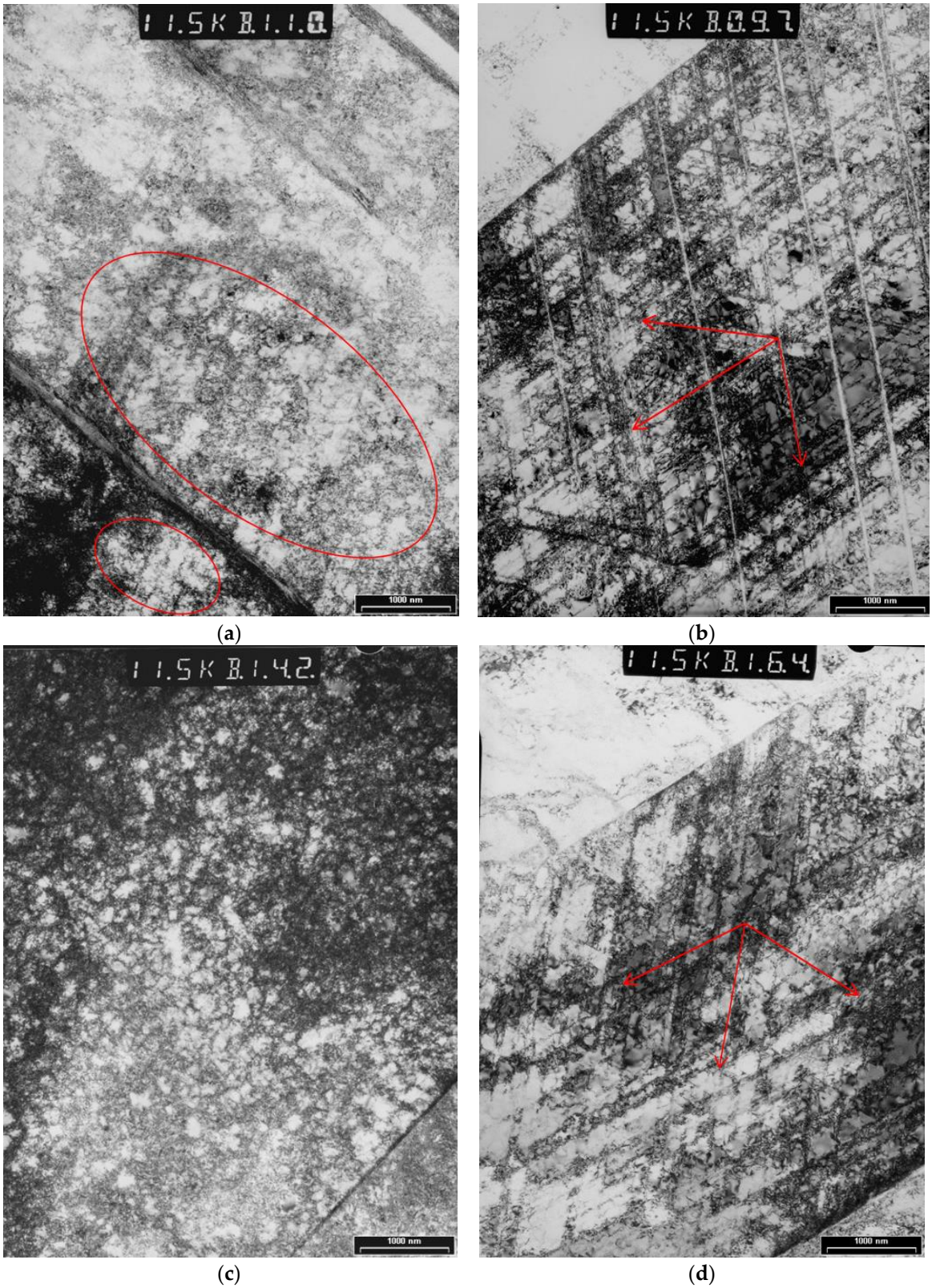

(**a**) (**b**)

(**c**) (**d**)

Figure 5. *Cont*.

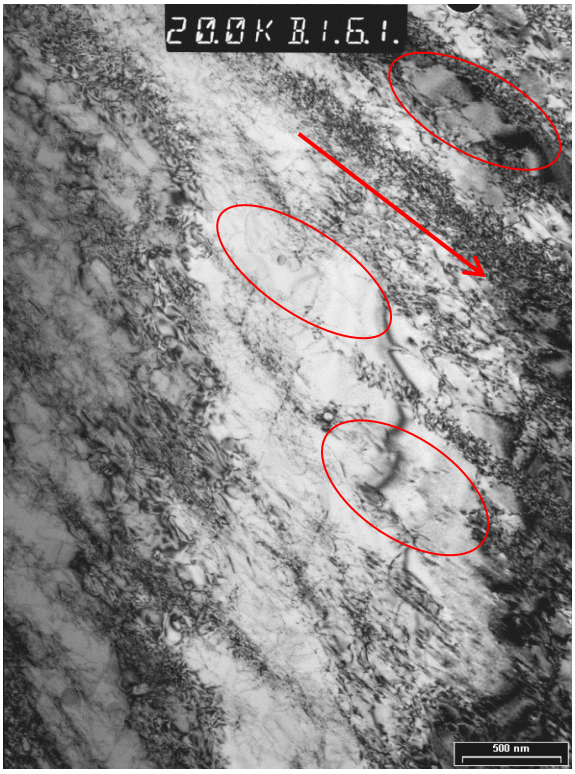

(**e**)

Figure 5. (**a**) TEM image of S31673, 14% CW taken from unloaded head of fatigue sample; (**b**) TEM image of CrMnN, 14% CW taken from unloaded head of fatigue sample; (**c**) TEM image of S31673, 14% CW taken from the gauge length of fatigued sample. (**d**) TEM image of CrMnN, 14% CW taken from the gauge length of fatigued sample. (**e**) TEM image of CrMnN, 14% CW taken from the gauge length of fatigued sample. No distinct glide bands are visible, but there is dislocation accumulation in one direction (red arrow). Red ellipses indicate the beginning of cell formation.

4. Conclusions

The fatigue behavior and the microstructural evolution during cyclic loading of the two austenitic stainless steel alloying concepts CrNi and CrMnN have been compared in the cold worked condition. For each concept, a representative alloy has been chosen. The CrMnN steel shows superior fatigue behavior, which is attributed to the high strength of the material caused by the interstitially alloyed nitrogen. The CrMnN grade showed a more pronounced reduction of the fatigue strength relating to $R_{p0.2}$ of the cold worked material than the CrNi grade (S31673). A possible explanation for that behavior could be found in the TEM investigations. S31673 showed a cellular dislocation structure which intensified during cyclic loading (see also Figure 1b) and characterises wavy slip. Conversely, the CrMnN grade demonstrated distinct planar dislocation glide, which has been proposed as a cause for dislocation annihilation [27], thus explaining the stronger reduction of the fatigue strength related to $R_{p0.2}$ during cyclic loading. An alternative explanation for the reduction of fatigue strength could be the strain localization on the surface through the planar dislocation glide in the CrMnN grade which can facilitates crack initiation.

Author Contributions: Conceptualization, R.F.; investigation, K.S.-H., M.B., and H.H.; methodology, R.F.; project administration, R.F.; resources, R.F.; supervision, M.K. and R.P.; visualization, R.F.; writing—original draft, R.F.; writing—review and editing, M.K., K.S.-H., and R.P.

Funding: This research received no external funding.

Conflicts of Interest: The authors declare no conflict of interest.

References

1. Feltner, C.E.; Laird, C. The role of slip character in steady state cyclic stress-strain behavior. *Trans. TMS-AIME* **1969**, *245*, 1372–1373.
2. Lukáš, P.; Klesnil, M. Dislocation structures in fatigued single crystals of Cu-Zn system. *Phys. Stat. Sol.* **1971**, *5*, 247–258. [CrossRef]
3. Mughrabi, H. Mikrostrukturelle Ursachen der Ermüdungsrissbildung. In *Ermüdungsverhalten Metallischer Werkstoffe, Symposium der Deutschen Gesellschaft für Materialkunde*; Bad Nauheim, Germany, 1984.
4. Mughrabi, H. Fatigue, an everlasting materials problem—Still en vogue. *Procedia Eng.* **2010**, *2*, 3–26. [CrossRef]
5. Uggowitzer, P.J. Stickstofflegierte Stähle. In *Ergebnisse der Werkstoffforschung*; Thubal-Kain: Zürich, Switzerland, 1991; pp. 87–101.
6. Simmons, J.W. Strain hardening and plastic flow properties of nitrogen-alloyed Fe-17Cr-(8–10) Mn-5Ni austenitic stainless steels. *Acta Mater.* **1997**, *45*, 2467–2475. [CrossRef]
7. Llewellyn, D.T. Work hardening effects in austenitic stainless steels. *Mater. Sci. Technol.* **1997**, *13*, 389–400. [CrossRef]
8. Kikuchi, M.; Mishima, Y. (Eds.) *High Nitrogen Steels HNS95*; ISIJ International: Kyoto, Japan, 1996.
9. Hänninen, H. Application and performance of high nitrogen steels. In *High Nitrogen Steels 2004*; GRIPS Media: Ostend, Belgium, 2004.
10. Fawley, R.; Quader, M.A.; Dodd, R.A. Compositional effects on the deformation modes, annealing twin frequencies, and stacking fault energies of austenitic stainless steels. *TMS AIME* **1968**, *242*, 771–778.
11. Schramm, R.E.; Reed, R.P. Stacking fault energies of seven commercial austenitic stainless steels. *Metall. Trans. A* **1975**, *6*, 1345–1351. [CrossRef]
12. Stoltz, R.E.; Sande, J.B.V. The effect of nitrogen on stacking fault energy of Fe-Ni-Cr-Mn steels. *Metall. Trans. A* **1980**, *11*, 1033–1037. [CrossRef]
13. Petrov, Y. *Defects and Diffusionless Transformation in Steel (Russian)*; Naukova Dumka: Kiew, Ukraine, 1978; p. 262.
14. Fujikura, M.; Takada, K.; Ishida, K. Effect of manganese and nitrogen on the mechanical properties of Fe-18%Cr-10%Ni stainless steels. *Trans. Iron Steel Inst. Jan.* **1975**, *15*, 464–469.
15. Mosecker, L.; Saeed-Akbari, A. Nitrogen in chromium–manganese stainless steels: A review on the evaluation of stacking fault energy by computational thermodynamics. *Sci. Technol. Adv. Mater.* **2013**, *14*, 033001. [CrossRef] [PubMed]
16. Razumovskiy, V.I.; Hahn, C.; Lukas, M.; Romaner, L. Ab Initio Study of Elastic and Mechanical Properties in FeCrMn Alloys. *Materials* **2019**, *12*, 1129. [CrossRef] [PubMed]
17. Lee, S.-J.; Fujii, H.; Ushioda, K. Thermodynamic calculation of the stacking fault energy in Fe-Cr-Mn-C-N steels. *J. Alloys Compd.* **2018**, *749*, 776–782. [CrossRef]
18. Douglas, D.L.; Thomas, G.; Roser, W.R. Ordering, Stacking Faults and Stress Corrosion Cracking In Austenitic Alloys. *Corrosion* **1964**, *20*, 15–28. [CrossRef]
19. Gerold, V.; Karnthaler, H.P. On the origin of planar slip in F.C.C. alloys. *Acta Metall.* **1989**, *37*, 2177–2183. [CrossRef]
20. Grujicic, M.; Nilsson, J.-O.; Owen, W.S.; Thorvaldsson, T. Basic deformation mechanisms in nitrogen strengthened stable austenitic stainless steels. In *High Nitrogen Steels, HNS 88*; The Institute of Metals: London, UK, 1988.
21. Gavriljuk, V.G.; Berns, H. *High Nitrogen Steels: Structure, Properties, Manufacture, Applications*; Springer-Verlag: Berlin/Heidelberg, Germany, 1999.
22. Ojima, M.; Adachi, Y.; Tomota, Y.; Katada, Y.; Kaneko, Y.; Kuroda, K.; Saka, H. Weak Beam TEM Study on Stacking Fault Energy of High Nitrogen Steels. *Steel Res. Int.* **2009**, *80*, 477–481.
23. Noh, H.; Kang, J.-H.; Kim, K.-M.; Kim, S.-J. Different Effects of Ni and Mn on Thermodynamic and Mechanical Stabilities in Cr-Ni-Mn Austenitic Steels. *Metall. Mater. Trans. A* **2019**, *50*, 616–624. [CrossRef]
24. Degallaix, S.; Foct, J.; Hendry, A. Mechanical behaviour of high-nitrogen stainless steels. *Mater. Sci. Technol.* **1986**, *2*, 946–950. [CrossRef]
25. Taillard, R.; Foct, J. Mechanisms of the action of nitrogen interstitials upon low cicle fatigue behaviour of 316 stainless steels. In *High Nitrogen Steels, HNS88*; The Institute of Metals: London, UK, 1988.

26. Panzenböck, M.H. Ermüdungsverhalten Stickstofflegierter Cr-Mn-Austenite. Ph.D. Thesis, University of Leoben, Leoben, Austria, 1995.
27. Degallaix, S. Role of nitrogen on the monotonic and cyclic plasticity of Type 316L SS at Room temperature. In *Basic Mechanisms in Fatigue of Metals*; Lukas, P., Polak, J., Eds.; Academia: Prague, Czech Republic, 1988; pp. 65–72.